

# Journal of Biomedical Optics

SPIEDigitalLibrary.org/jbo

## **Time-resolved imaging refractometry of microbicial films using quantitative phase microscopy**

Matthew T. Rinehart  
Tyler K. Drake  
Francisco E. Robles  
Lisa C. Rohan  
David Katz  
Adam Wax



# Time-resolved imaging refractometry of microbicidal films using quantitative phase microscopy

Matthew T. Rinehart,<sup>a</sup> Tyler K. Drake,<sup>a</sup>  
Francisco E. Robles,<sup>a</sup> Lisa C. Rohan,<sup>b</sup>  
David Katz,<sup>c</sup> and Adam Wax<sup>a</sup>

<sup>a</sup>Duke University, Department of Biomedical Engineering, Fitzpatrick Institute for Photonics, 3000 Science Drive, 136 Hudson Hall, Box 90281, Durham, North Carolina 27708

<sup>b</sup>University of Pittsburgh, School of Pharmacy, Magee Womens Research Institute, Pittsburgh, Pennsylvania 15213

<sup>c</sup>Duke University, Department of Biomedical Engineering, Center for Biomolecular and Tissue Engineering, 136 Hudson Hall, Box 90281, Durham, North Carolina 27708

**Abstract.** Quantitative phase microscopy is applied to image temporal changes in the refractive index (RI) distributions of solutions created by microbicidal films undergoing hydration. We present a novel method of using an engineered polydimethylsiloxane structure as a static phase reference to facilitate calibration of the absolute RI across the entire field. We present a study of dynamic structural changes in microbicidal films during hydration and subsequent dissolution. With assumptions about the smoothness of the phase changes induced by these films, we calculate absolute changes in the percentage of film in regions across the field of view. © 2011 Society of Photo-Optical Instrumentation Engineers (SPIE). [DOI: 10.1117/1.3665439]

Keywords: quantitative phase microscopy; microbicides; microbicidal films; interferometry; refractometry; imaging; refractive index.

Paper 11545LR received Sep. 26, 2011; revised manuscript received Nov. 9, 2011; accepted for publication Nov. 14, 2011; published online Dec. 19, 2011.

Microbicides are topical products that are designed to reduce the risk of HIV/AIDS transmission and can be deployed *in vivo* using various delivery forms, such as films, gels, tablets, ring devices, or injections.<sup>1</sup> Although each of these dosage forms has advantages and drawbacks, they are all designed to provide discreet protection from HIV that young women, who are 3–5× more likely to be infected than men, can use independently and proactively.<sup>1</sup> Recently, thin polymeric films have been evaluated as delivery vehicles for microbicidal active pharmaceutical ingredients (APIs).<sup>2</sup> Microbicidal films are heterogeneous sheets ranging from tens to hundreds of microns in thickness and typically contain APIs, water soluble polymers, and plasticizers (e.g., cholesterol, ethanol, carbopol, etc.).<sup>2</sup> Depending on their composition, these films can exhibit highly variable hydration profiles and dissolution dynamics. Because

these films are designed to prevent aqueous degradation of the API by hydrating only after topical application, the parameters that characterize API release include inherent moisture content, disintegration time, dynamic hydration rates, and drug-content uniformity. Current methods of film assessment include bulk physical, chemical, and mechanical testing on a macroscopic scale; however, microscopic investigation of film dissolution has not been previously conducted and could be used to inform the compositions of clinical microbicidal films.

Quantitative phase microscopy (QPM) is well adapted to imaging microbicidal film solutions. The method is based on recording the complex amplitude and phase of light that is transmitted through a sample with weak refractive index (RI) variations, which gives rise to relative optical path length changes. We have previously developed QPM as a tool for imaging various cell types and studying dynamic biological phenomena.<sup>3,4</sup> Other studies of imaging cell samples have sought to decouple optical thickness from RI in phase measurements using various approaches,<sup>5–8</sup> however these methods and their assumptions are not necessarily applicable to studying microbicidal films that dissolve over time. Therefore, to enable effective studies of film dissolution dynamics, an alternative method of determining absolute RI is needed with a single measurement in time preferred.

In this letter, we present the novel method of using a sloped physical calibration structure in QPM imaging to facilitate accurate calculation of the absolute RI from measured optical path lengths. We use a set chamber thickness and a calibration standard, a polydimethylsiloxane (PDMS) ramp fabricated by soft lithography, in the field of view (FOV) to determine the absolute RI of the sample at every two-dimensional spatial location using only a single temporal acquisition. On the basis of the assumptions of smoothness in the phase variations over time and the final spatial distribution, the PDMS ramp allows straightforward calculation of the absolute RI without sensitivity to temporal phase drift. To demonstrate the utility of this technique, we use this novel time-resolved imaging refractometer to image temporal changes in the RI distributions of solutions created by microbicidal films undergoing hydration.

Quantitative phase maps are acquired using an interferometric microscopy system similar to that previously described in Ref. 9, but with slight modifications. In the present experiments, we use a 532-nm laser (LaserGlow Technologies, Toronto, Canada) for illumination. The sample consists of a flow chamber (FCS3 chamber, Biopetech, Butler, Pennsylvania) with No. 1 coverslips as upper and lower surfaces at a fixed physical thickness determined by an intermediate spacer (250 μm nominal thickness), and inlet/outlet ports to allow fluid flow. Transmitted light through the sample and reference arms of the interferometer is collected with matched 10x objectives (“A-Plan” 0.25NA, Carl Zeiss Microscopy, Thornwood, New York) and recombined prior to being imaged by an  $f = 150$  mm achromatic tube lens onto a CCD (CoolSNAP *cf* 1392 × 1040 pixels, Photometrics, Tuscon, Arizona). The use of identical objectives allows us to minimize curvature mismatch of the optical wavefronts; these are arranged to produce a linear off-axis interference pattern,

Address all correspondence to: Matthew T. Rinehart, Duke University, Department of Biomedical Engineering, Fitzpatrick Institute for Photonics, 3000 Science Drive, 136 Hudson Hall, Box 90281, Durham, North Carolina 27708. Tel: 919-210-2051; Fax: 919-613-9144; E-mail: matt.rinehart@duke.edu.

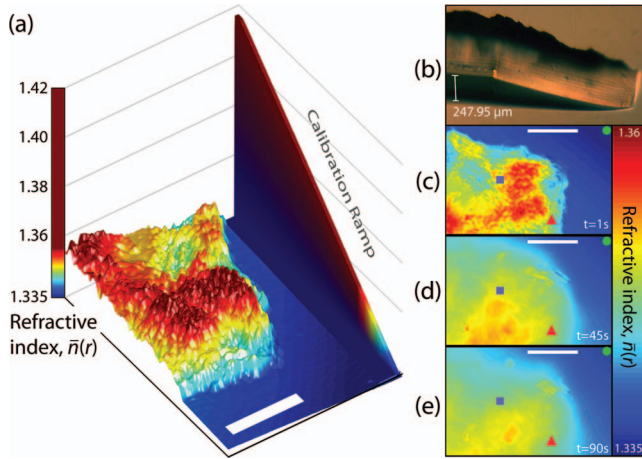


**Fig. 1** Two-dimensional absolute refractive index maps of a CSIC film during dissolution at (a, c)  $t = 1$  s, (d)  $t = 45$  s, and (e)  $t = 90$  s. Scale bar represents  $200 \mu\text{m}$ . (b) Representative image of the PDMS calibration ramp. Plots in Fig. 2 come from the purple squares, red triangles, and green circles seen in (c–e). (a) is a still image from Video 1 (QuickTime, 6.2 MB). [URL: <http://dx.doi.org/10.1117/1.3665439.1>]

which may be optimized by axially and laterally adjusting the reference arm objective and its incident beam.

This QPM system records off-axis interferograms, which are processed to produce phase maps by spatially filtering to remove the complex conjugate and autocorrelation terms, and then recentering in Fourier space. Inverse Fourier transformation of the result yields the complex wavefront at the image plane. After taking the angle of the complex data, the resulting phase information is unwrapped using a combined temporal<sup>10</sup> and spatial<sup>11</sup> method to produce three-dimensional data sets free of  $2\pi$  ambiguities. Under assumptions of temporal and spatial smoothness (i.e., the phase between two adjacent data points is not more than  $\pi$ ), the following phase unwrapping algorithm is employed (i) use a one-dimensional unwrapping algorithm to temporally unwrap the phase of each lateral pixel; (ii) use a two-dimensional quality map-guided algorithm to unwrap the phase of the last frame; and (iii) add the unwrapped phase from the last frame to each of the previous frames that have been temporally unwrapped in a pointwise fashion. This phase unwrapping method yields unambiguous phase images over an extended time-course experiment, but requires further analysis to determine the absolute RI.

Relative optical path delays,  $D_R(\mathbf{r})$ , across a FOV as well as the average RI,  $\bar{n}$ , are related to the measured relative phase shifts,  $\varphi_R$ , as  $D_R(\mathbf{r}) = \varphi_R(\mathbf{r}) \frac{\lambda}{2\pi} = \bar{n}(\mathbf{r})d$ , where  $d$  is the total thickness of the chamber. From this expression, the relative RI can be calculated. However, the measured phase only accounts for relative path differences across the FOV. One approach to obtaining the absolute RI is to introduce some known landmark into the FOV that can be used to aid unwrapping within the area of interest. As a reference, we used a molded polydimethylsiloxane (PDMS) ramp structure [Fig. 1(b)] with a maximum height that was matched to the sample chamber spacer thickness and a ramp length that almost spans the width of the interferometric microscope's FOV. After being UV-epoxied to the lower coverslip of the chamber, the ramp makes contact with the up-

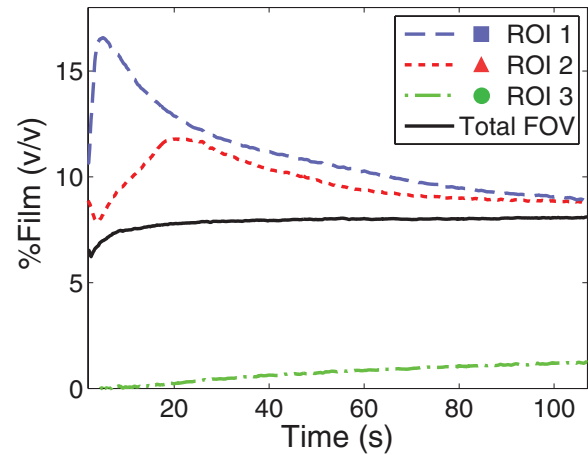


**Fig. 2** Time-resolved dissolution curves of the volume fraction percentages (v/v) of film within the integral depth over an ROI. ROIs 1–3 are  $100\text{-}\mu\text{m}^2$  areas taken at the markers in Figs. 1(c)–1(e).

per coverslip at the thickest section of PDMS, providing a fixed thickness and constant RI reference. By placing the ramped edge in the FOV [Fig. 1(a)], the absolute RI across the FOV is calibrated by adding the difference between  $\bar{n}(\mathbf{r})$  at the top of the PDMS ramp and the previously measured RI of PDMS to the relative RI distribution of each frame. This provides a constant phase reference in each frame that eliminates temporal phase drift from our measurements.

To calibrate the PDMS ramp as an absolute RI reference, we experimentally verified both the height and RI of these structures. The maximum ramp height was measured to be  $247.95 \pm 0.01 \mu\text{m}$  using a 3-D optical surface profiler (NewView 5000, ZYGO, Middlefield, Connecticut). The exact RI of the PDMS ramp at  $\lambda = 532 \text{ nm}$  was determined by immersing the structure in set mixtures of water and glycerol and measuring each with our QPM setup. RI measurements,  $\bar{n}(\mathbf{r})$ , were calculated from the unwrapped phase profiles of the ramp,  $\varphi_R(\mathbf{r})$ , using the total chamber height  $d = 247.95 \mu\text{m}$ . The mean RI of this PDMS ramp as determined by multiple measurements was found to be 1.4166 with a standard deviation of  $4.1 \times 10^{-4}$ . The refractive indices of the immersion media were measured at  $\lambda = 589.3 \text{ nm}$  using a commercial bulk-fluid refractometer (RFM 340, Bellingham & Stanley) and then corrected for temperature ( $22.4^\circ\text{C}$ ) and wavelength using the dispersion characteristics of water and glycerol.<sup>12–14</sup> The achievable precision of relative temporal and spatial changes in RI was determined by measuring the standard deviation of temporal phase fluctuations. Repeated imaging [100 frames at 10 frames per second (fps)] of a  $100\text{-}\mu\text{m}^2$  region of water produced phase fluctuations corresponding to an RI variation of  $5.5 \times 10^{-6}$ . In comparison, any phase unwrapping complications that add incorrect multiples of  $2\pi$  to the phase maps cause RI errors in multiples of  $2.15 \times 10^{-3}$ .

To characterize microbicidal film dissolution, quantitative phase images were acquired at a rate of 10 fps over 106 s. The film was a custom formulation loaded with API 5-chloro-3-phenylsulfonylindole-2-carboxamide (CSIC), a hydrophobic non-nucleoside reverse transcriptase inhibitor with potent activity against HIV. The CSIC-containing film had previously been characterized to be 0.076 mm thick with an

average water content of 7.33%; it also had an average refractive index of 1.4699, which was determined using the relative dispersion profile measured by a method similar to that described in Ref. 15 and a reference RI measurement taken at  $\lambda = 589.3$  nm using a commercial bulk fluid refractometer (RFM 340, Bellingham & Stanley). The film was loaded into the flow chamber with the calibration ramp at the edge of the FOV and enclosed with a top coverslip. At time  $t = 0$ , water was injected into one port of the flow chamber until both the ramp and film were fully immersed. After immersion, water flow was ceased in order to limit the dynamic behavior of the system to diffusion dynamics. Figure 1(a) shows the two-dimensional absolute RI mapping of both the calibration ramp and film at a time point 1 s after immersion. As can be visualized in Fig. 1(c)–1(e) and Video 1, the film was initially very granular. During hydration and dissolution, the film spread laterally and evolved toward a more uniform refractive index distribution.

The volume fraction percentages of film and water at a specific point in the FOV were calculated by decomposing the measured RI,  $\bar{n}(\mathbf{r})$ , as a linear combination of the bulk film RI,  $n_f$ , and the RI of water,  $n_{\text{H}_2\text{O}}$ , which had been measured to be 1.4699 and 1.3351, respectively. Figure 2 shows the volume fraction percentages (% v/v) of film at three different 100- $\mu\text{m}^2$  regions of interest (ROIs), as indicated by the corresponding colored squares in Fig. 1(c)–1(e), and also for the entire FOV. Relatively fast changes occurred in the first 10 s of dissolution, and the system gradually progressed toward a more uniform distribution of film and water over the full 106 s time course. The total amount of film in the FOV also increased gradually during this process as shown by the solid black curve in Fig. 2. As seen from the changes in ROI 3, which is farthest from the film at initial hydration, the percent of film increased from 0 to 1.240%. Without the use of the PDMS calibration ramp, it would be impossible to decouple this change from the temporal phase drift of the optical system and both the average integral RI measurements and percent film calculations would be inaccurate. As defined by the standard deviations of the PDMS RI measurements described above, the absolute film percentages shown in Fig. 2 have an accuracy of 0.3 percentage points (pp) and a precision of 0.004 pp.

In summary, we have presented a novel method of time-resolved imaging refractometry based on QPM. Both two-dimensional spatial phase unwrapping and pointwise temporal phase unwrapping were combined to remove phase ambiguities from the complete data set. By using a set chamber thickness and a physical calibration ramp structure in the FOV, the system is immune to temporal drift and we are able to calculate not only relative but also absolute RI. These measurements are accurate to  $\sigma = 4.1 \times 10^{-4}$ , and the relative changes in RI are bounded by a standard deviation of  $\sigma = 5.5 \times 10^{-6}$ . This technique is a highly accurate measurement tool that can be used to image RI distributions as a function of time for a variety of transparent samples. It should be noted that while a frame rate of 10 fps was sufficient to investigate the dynamics of film dissolution in this study, it is also possible to use this method at higher speeds and it is only limited by the camera acquisition rate and illuminating power level. The spatial and temporal film dissolution profiles obtained

with this method can be used to model the transport of APIs into tissue. We anticipate that this measurement approach will be useful for evaluating the diffusion characteristics of various film compositions and optimizing their overall effectiveness.

### Acknowledgments

We gratefully acknowledge help in the photolithography process provided by the Duke University Shared Materials Instrumentation Facility. This work was supported by grants from the National Institutes of Health (NIH) (No. NCI 1 R01 CA138594-01 and No. U19-AI 077289), the NIH National Institute of Allergy and Infectious Disease (NIAID) (No. AI082639, No. AI079801, and No. AI082623), and the National Science Foundation (No. MRI-1039562).

### References

1. A. Stone and P. F. Harrison, *Microbicides: Ways Forward*, Alliance for Microbicide Development, Silver Spring, MD (2010).
2. S. Garg, D. Goldman, M. Krumme, L. C. Rohan, S. Smoot, and D. R. Friend, "Advances in development, scale-up and manufacturing of microbicide gels, films, and tablets," *Antiviral Res.* **88**, S19–S29 (2010).
3. N. T. Shaked, Y. Zhu, M. T. Rinehart, and A. Wax, "Two-step-only phase-shifting interferometry with optimized detector bandwidth for microscopy of live cells," *Opt. Express* **17**, 15585–15591 (2009).
4. N. T. Shaked, M. T. Rinehart, and A. Wax, "Dual-interference-channel quantitative-phase microscopy of live cell dynamics," *Opt. Lett.* **34**, 767–769 (2009).
5. B. Rappaz, F. Charrière, C. Depeursinge, P. J. Magistretti, and P. Marquet, "Simultaneous cell morphometry and refractive index measurement with dual-wavelength digital holographic microscopy and dye-enhanced dispersion of perfusion medium," *Opt. Lett.* **33**, 744–746 (2008).
6. B. Rappaz, P. Marquet, E. Cuche, Y. Emery, C. Depeursinge, and P. J. Magistretti, "Measurement of the integral refractive index and dynamic cell morphometry of living cells with digital holographic microscopy," *Opt. Express* **13**, 9361–9373 (2005).
7. B. Kemper, S. Kosmeier, P. Langehanenberg, G. von Bally, I. Bredebusch, W. Domschke, and J. Schnekenburger, "Integral refractive index determination of living suspension cells by multifocus digital holographic phase contrast microscopy," *J. Biomed. Opt.* **12**, 054009 (2007).
8. N. Lue, G. Popescu, T. Ikeda, R. R. Dasari, K. Badizadegan, and M. S. Feld, "Live cell refractometry using microfluidic devices," *Opt. Lett.* **31**, 2759–2761 (2006).
9. M. T. Rinehart, N. T. Shaked, N. J. Jenness, R. L. Clark, and A. Wax, "Simultaneous two-wavelength transmission quantitative phase microscopy with a color camera," *Opt. Lett.* **35**, 2612–2614 (2010).
10. J. M. Huntley and H. Saldner, "Temporal phase-unwrapping algorithm for automated interferogram analysis," *Appl. Opt.* **32**, 3047–3052 (1993).
11. D. Ghiglia and M. Pritt, *Two Dimensional Phase Unwrapping: Theory Algorithms & Software*, Wiley, Hoboken, NJ (1998).
12. P. Schiebener, J. Straub, J. M. H. Levelt Sengers, and J. S. Gallagher, "Refractive index of water and steam as function of wavelength, temperature and density," *J. Phys. Chem. Ref. Data* **19**, 677–717 (1990).
13. J. Rheims, J. Köser, and T. Wriedt, "Refractive-index measurements in the near-IR using an Abbe refractometer," *Meas. Sci. Technol.* **8**, 601–605 (1997).
14. L. F. Hoyt, "New table of the refractive index of pure glycerol at 20°C," *Ind. Eng. Chem.* **26**, 329–332 (1934).
15. F. E. Robles, L. L. Satterwhite, and A. Wax, "Non-linear phase dispersion spectroscopy," *Opt. Lett.* **36**(23), 4665–4667 (2011).